Spectroscopic Distribution of Dissolved Organic Matter in a Dam Reservoir Impacted by Turbid Storm Runoff

Jin Hur · Nahm-Chung Jung · Jae-Ki Shin

Abstract Spectroscopic characteristics of dissolved organic matter (DOM) in a large dam reservoir were determined using ultraviolet absorbance and fluorescence spectroscopy to investigate spatial distribution of DOM composition after turbid storm runoff. Water samples were collected along a longitudinal axis of the reservoir at three to four depths after a severe storm runoff. Vertical profiles of turbidity data showed that a turbid water layer was located at a middle depth of the entire reservoir. The spectroscopic characteristics of DOM samples in the turbid water layer were similar to those of terrestrial DOM, as demonstrated by the higher specific UV absorbance (SUVA) and the lower fluorescence emission intensity ratio (F_{450}/F_{500}) compared to other surrounding DOM samples in the reservoir. Synchronous fluorescence spectroscopy revealed that higher content of humic-like DOM composition was contained in the turbid water. Fluorescence excitation–emission matrix (EEM) showed that lower content of protein-like aromatic amino acids was present in the turbid water

DOM. The highest protein-like fluorescence was typically observed at a bottom layer of each sampling location. The bottom water DOM exhibited extremely high protein-like florescence near the dam site. The particular observation was attributed to the low water temperature and the isolation of the local bottom water due to the upper location of the withdrawal outlet near the dam. Our results suggest that the distribution of DOM composition in a dam reservoir is strongly influenced by the outflow operation, such as selective withdrawal, as well as terrestrial-origin DOM inputs from storm runoff.

J. Hur
Department of Earth and Environmental Science,
Sejong University,
Seoul 143-747, South Korea

N.-C. Jung · J.-K. Shin (✉)
Korea Institute of Water and Environment,
Korea Water Resources Corporation,
Daejeon 305-730, South Korea
e-mail: jaekishin@kowaco.or.kr

1 Introduction

Most multi-purpose large dam reservoirs in Korea are surrounded by mountains and the water quantity and the quality are strongly influenced by the geologic and the hydrologic characteristics of the mountainous catchments as well as the local seasonal precipitation. Annual precipitation of Korea is approximately 1,280 mm/yr, half of which occurs primarily during the summer monsoon season (Kim et al. 2000). Due to the intense rainfall for a short period of time

(i.e., flash flooding), it is often reported that a significant amount of turbid (or muddy) water containing clay to silt-sized particles is input into dam reservoirs from the catchments (Shin et al. 2004). Currently, the turbid water is being recognized as a serious environmental problem in Korea and other Asian countries from the aspects of water resources management as well as drinking water treatment (Chen et al. 2006). The turbid storm runoff inflowing into reservoirs finally forms a separate layer at a middle depth (metalimnion) of reservoirs due to its relatively high density (Chen et al. 2006; Shin et al. 2004). The turbid runoff is known to supply massive quantities of organic carbon and nutrients to reservoirs (Kim et al. 2000; Shin et al. 2004).

Dissolved organic matter (DOM) is a heterogeneous mixture of constituents having a wide range of physicochemical properties (Thurman 1985). Ubiquitous in natural waters, DOM is composed of carbohydrates, proteins, lignins, and organic acids, and various other naturally occurring polymers. DOM plays a role in aquatic ecosystems as an important energy source for heterotrophic microorganisms (Steinberg 2003). It affects the acidity and the photochemistry of aquatic systems as well as the transport of organic and inorganic chemicals. DOM is also involved in the cycling of the trace element such as iron via the complexation. In drinking water treatments, DOM is known to be precursors of disinfection by-products and it may also cause detrimental problems on filtration processes such as membrane fouling (Her et al. 2004).

DOM in lake water is typically classified into two types by its source. Allochthonous DOM, composed of terrestrial humic substances, is supplied by runoff from the surrounding catchments. The quantity and the quality of allochthonous DOM depend on the characteristics of the surrounding watershed such as the vegetation type, the hydrology and the geochemistry. Autochthonous DOM is produced from in-lake processes, mainly from carbon excretion of phytoplankton, leachate of dead algal cells and microbial degradation. In general, major components of allochthonous DOM are recalcitrant, humic-like and highly colored compounds, whereas autochthonous DOM is susceptible to microbial alternations in aquatic environments (McKnight et al. 2001). The apparent physicochemical properties of DOM in a lake are altered by microbial transformations and photochemical degradation as well as the mixing processes of DOMs of different origin (Wetzel 2001).

Although it is known that allochthonous input of DOM is much lower than autochthonous production in large lakes (Wetzel 2001), the relative contribution of the two different DOM end members to the lake carbon budget depends on the hydraulic retention time, the trophic state, and the development of the littoral zone. In fact, a particular event of turbid water runoff may act as a major contributor to the allochthonous input of DOM in lakes, affecting the carbon cycles of the lakes. For example, Kim et al. (2000) estimated that storm runoff during the summer monsoon contributed approximately 87% of the total allochthonous carbon loading to Lake Soyang, a typical dam reservoir in Korea, during the summer monsoon period from July to August, 1996. There is no doubt that distribution of DOM composition is strongly affected by inflowing turbid water runoff in a reservoir. Surprisingly, however, almost no study has been conducted to investigate variations of DOM composition due to the turbid water input.

Ultraviolet–visible (UV–vis) and fluorescence spectroscopic techniques have been widely applied to characterize DOM. Although the spectroscopic techniques may elucidate only a limited carbon structures of DOM (e.g., UV-absorbing moieties and fluorescent organic matters), numerous previous studies suggest that several DOM types and the composition can be adequately addressed by comparing some selected spectroscopic characteristics. For example, Battin (1998) used the absorbance ratio of A_{254}/A_{436} to estimate the relative composition of autochthonous DOM versus terrestrial DOM. Miano and Senesi (1992) have shown that synchronous fluorescence peaks at shorter wavelengths represent fulvic acid fractions associated with a lower degree of aromaticity, whereas the peaks appearing at longer wavelengths represent polycondensation of phenolic aromatic components such as humic acids. In addition, peak intensities in different locations of fluorescence excitation–emission matrix (EEM) have been used to probe protein-like materials (i.e., labile DOM), humic acids and fulvic acids of DOM in rivers, lakes and oceans. For example, Baker (2001) utilized a peak ratio of protein-like fluorescence to fulvic-like fluorescence to discriminate sewage-impacted river water from water without the impact.

Recently, Hur et al. (2006) compared several fluorescence discrimination indices previously reported using well-defined mixtures of a terrestrial DOM and an aquatic DOM and they demonstrated that a fluorescence peak ratio corresponding to humic-like versus fulvic-like regions was best suitable to distinguish terrestrial DOM composition from the mixtures of the two end member DOMs.

Although the described spectroscopic techniques have been successfully employed for tracking changes in the distribution of DOM composition in rivers (Baker 2001; McKnight et al. 2001), natural lakes (Balogh et al. 2003; Hayakawa et al. 2004; McKnight et al. 2001; Wu et al. 2003) and oceans (Coble 1996; Jaffé et al. 2004; Parlanti et al. 2000), they have been scarcely applied in dam reservoirs. It should be noted that no attempt was made in this study to link any spectroscopic parameters with tracing DOM sources and/or estimating the contribution of different sources to dam reservoirs. Our interest here was to illustrate the distribution of DOM composition in a dam reservoir with a sporadic input of turbid storm water using some previously-known spectroscopic techniques, which include specific UV absorbance (SUVA), UV absorbance ratio (A_{254}/A_{436}), fluorescence emission intensity ratio (F_{450}/F_{500}), synchronous fluorescence spectroscopy, and fluorescence EEM.

2 Materials and Methods

2.1 Site description

The Yongdam Reservoir is a typical large dam reservoir located on the upper Geum river basin in southwestern Korea (E127° 31′ 40″, N35° 56′ 30″), which is one of four largest river basins in Korea. The dam reservoir was flooded on December 24, 2001. It is a long and narrow dentritic type reservoir with a total length of approximately 30 km and a total storage volume of 5.1×10^8 m^3. The trophic state of the reservoir is classified into eutrophic to mesotrophic, depending on the season and the location. The average rainfall in this region for 2004–2005 was 1,420 mm/year. Likewise in other regions of Korea, intense rainfall occurs in the area

primarily during the summer monsoon season from July to August, which contributes nearly half of the total rain amount in a year. The total amount of the rainfall in July and August is estimated to be 47% of the annual precipitation for the year 2004. The overall land use/cover in the Yongdam Reservoir watershed is 68% forest, 30% agriculture, and 1.7% urban area. Five major rivers flow into the reservoir from the surrounding hills (Fig. 1). The combined inflow from the three rivers (A, B, and C) reaches 74% of the total amount of the inflow from the five rivers into the reservoir. The annual average inflow of all the rivers to the reservoir is 31.2 m^3/s with a large temporal variation (Fig. 2). However, the outflow rate remains relatively stable, following the dam purposes and the operation. For the Yongdam Reservoir, water is discharged through the withdrawal outlet of the intake tower near the dam (Fig. 3). The outlet is operated to withdraw only the upper layer water of the reservoir at the depth from 0 to 8 m. Vascular plants in the littoral zone are not well developed because of dramatic changes in water level in response to increases of rainfall in the summer monsoon.

2.2 Materials

Four locations were selected along a main axis of the Yongdam Reservoir from the reservoir upstream to the dam site (Fig. 2). Turbid water phenomenon was reported at dam of the reservoir immediately after a severe storm event on July 1, 2005, resulting in a sharp increase of the reservoir storage volume (Personal communication from the regional office of Korea Water Resources Corporation for the Yongdam Reservoir). After the severe storm runoff, another rain event occurred on July 12, which is likely to affect the water quality of the reservoir as well. Sampling was conducted on July 25, 2005, which corresponds to 24 days after the first severe storm event.

Water samples were collected with a Van Dorn sampler (3 L) at the selected sampling locations, with three to four depths (the upper, the middle, turbid water, and the bottom layers). The depth of the turbid water layer corresponds to the maximum turbidity value at each location. The sampling depths for each location were given in Table 1. Rainfall, water inflow, outflow and elevation data were obtained from Korea
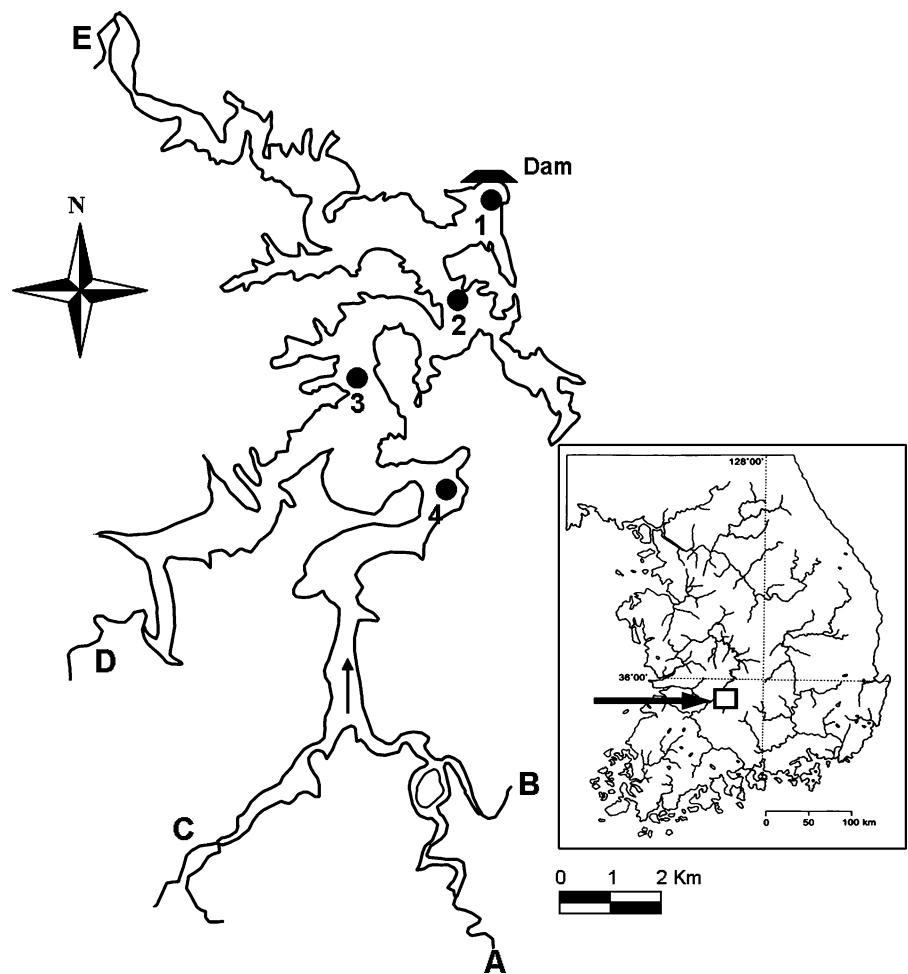
Water Resources Corporation (KOWACO). At each sampling location, depth profiles of temperature, conductivity, pH, dissolved oxygen (DO) and turbidity were measured with a YSI 6,600 m (Yellow Spring Instrument, USA). Suwannee River fulvic acid (SRFA), Suwannee River humic acid (SRHA), Elliott soil humic acid (SHA) were obtained from the International Humic Substances Society (IHSS) and used without further purification. All IHSS materials were dissolved in distilled, deionized water (DDW) and stored at 4°C at concentrations of approximately 5 mg C/L. The collected samples were filtered (pre-ashed Whatman GF/F microfiber filter paper, Whatman, West Chester, PA) and acidified with 1N HCl to pH 3 to quantify the dissolved organic carbon (DOC) concentration and to obtain the spectroscopic characteristics. No precipitates were observed with the samples at pH 3. It is previously recommended that

field DOM samples should be acidified to pH 3 for fluorescence measurements because the low pH can minimize potential complexation between DOM and metals (Westerhoff et al. 2001).

2.3 Analytical methods

DOC concentrations in sample filtrates were measured by TOC analyzer (Tekmar Dohrman, Phoenix 8000). All DOC samples were acidified and purged with nitrogen to eliminate the inorganic carbon. The relative precision of the DOC analysis was <3% as determined by repeated measurements. Absorption spectra (resolution of 1 nm) of the DOM samples over the wavelength range 200–600 nm were measured by a UV–vis spectrophotometer (Cary 300 Conc, Varian) using a 1 cm quartz cuvette. A blank solution (Milli-Q water) was used as a reference for the absorption

Fig. 2 Seasonal variations of daily rainfall, inflow rate, outflow rate, and water level in the Yongdam Reservoir (2004–2005) before the sampling date. The water level was 254.0 m elevation on the sampling date. The *vertical arrows* indicate the sampling date
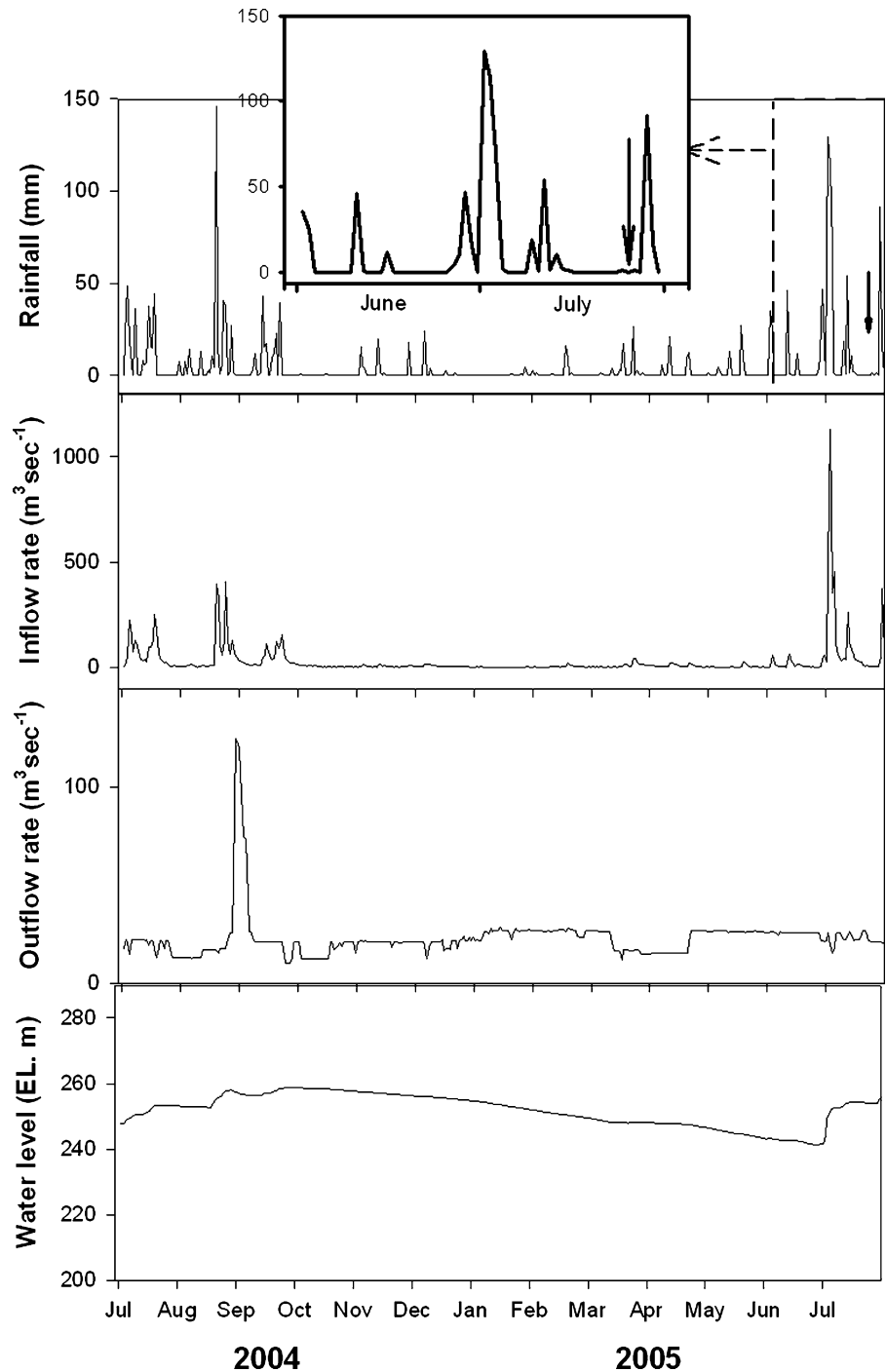
measurements. The SUVA value of each filtered sample was determined by dividing the UV absorbance of the sample at 254 nm with the DOC and multiplying the ratio by 100. The fluorescence spectra of the filtered DOM samples were recorded using a luminescence spectrometer (Perkin–Elmer LS-55) equipped with a 20 kW xenon arc lamp. Aliquots of the samples were diluted prior to the fluorescence measurements until UV absorbance at 254 nm was below 0.1 to avoid the inner-filter correction (Alberts

Fig. 3 Schematic representation of the Yongdam dam reservoir and the water movement through the withdrawal outlet. The *arrows* indicate the direction of the water movement
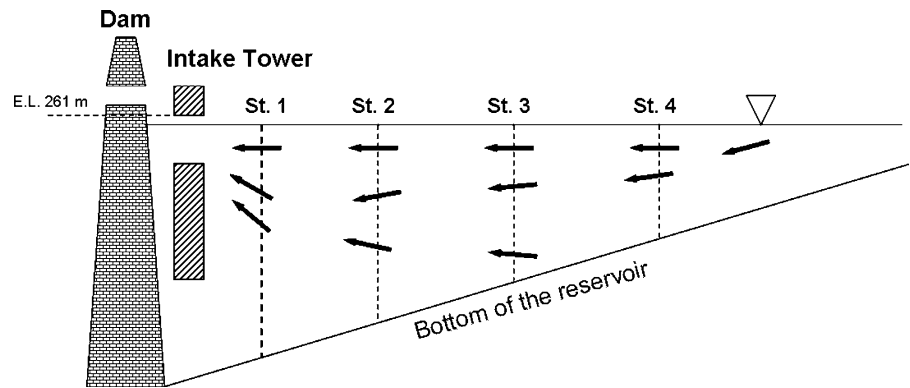
and Takács 2004; Mobed et al. 1996). Excitation and emission slits were adjusted to 10 and 5 nm, respectively. To limit second-order Raleigh scattering, a 290-nm cutoff filter was used for all the fluorescence measurements. The measured fluorescence intensities were standardized to a Raman peak (143 unit for this study) at 395 nm emission (Baker 2001). Three types of fluorescence measurements were made for each sample-emission spectrum, synchronous spectrum, and fluorescence EEM. First, emission

spectra were measured at an excitation wavelength of 370 nm to obtain fluorescence index (McKnight et al. 2001). Next, synchronous fluorescence spectra for excitation wavelengths ranging from 300 to 600 nm were recorded using a constant offset ($\Delta\lambda=30$ nm) between excitation and emission wavelengths. To obtain fluorescence EEMs, the fluorescence intensity was measured for excitation wavelengths ranging from 200 to 400 nm and for emission wavelengths ranging from 280 to 580 nm, using 5-nm and 0.5-nm

Table 1 UV–vis and fluorescence spectroscopic characteristics of the Yongdam Reservoir DOM samples and IHSS standard DOM

Sampling locations or IHSS DOM	Depth (m)	Turbidity (NTU)	UV–vis spectroscopy			Fluorescence spectroscopy		
			SUVA (L/ mg C)	A_{254}/A_{436}	F_{450}/F_{500}	Humic-like/ fulvic-like[a]	Protein-like fluorescence[b]	Protein-like/ humic-like[b]
Station 1	5.0	3.3	2.54 (0.09)[c]	15.08 (0.43)	1.89 (0.05)	0.14 (0.004)	20.4 (0.74)	2.23 (0.06)
	15.3	95.1	7.65 (0.28)	5.24 (0.15)	1.66 (0.05)	0.30 (0.008)	16.7 (0.60)	0.62 (0.02)
	25.5	7.6	2.57 (0.09)	16.71 (0.47)	1.85 (0.05)	0.16 (0.005)	7.9 (0.28)	1.35 (0.04)
	42.0	3.0	2.43 (0.09)	19.72 (0.56)	1.90 (0.05)	0.14 (0.004)	105.5 (3.80)	12.3 (0.35)
Station 2	5.0	2.5	3.05 (0.11)	13.57 (0.38)	1.86 (0.05)	0.15 (0.004)	11.3 (0.41)	1.02 (0.03)
	13.7	94.3	7.19 (0.26)	5.83 (0.16)	1.65 (0.05)	0.30 (0.008)	9.65 (0.35)	0.62 (0.02)
	30.3	64.5	8.27 (0.30)	5.08 (0.14)	1.63 (0.05)	0.29 (0.008)	12.1 (0.44)	0.60 (0.02)
	35.2	3.6	2.40 (0.09)	24.79 (0.70)	1.87 (0.05)	0.14 (0.003)	13.3 (0.48)	1.40 (0.04)
Station 3	5.0	1.6	2.83 (0.10)	14.28 (0.40)	1.90 (0.05)	0.17 (0.005)	10.36 (0.37)	0.94 (0.03)
	14.9	78.1	7.21 (0.26)	6.8 (0.19)	1.70 (0.05)	0.29 (0.008)	9.95 (0.36)	0.55 (0.02)
	24.6	14.4	5.39 (0.19)	13.25 (0.37)	1.83 (0.05)	0.16 (0.005)	11.5 (0.42)	1.18 (0.03)
Station 4	5.0	5.0	2.45 (0.09)	11.24 (0.32)	1.86 (0.05)	0.17 (0.005)	13.1 (0.47)	1.00 (0.03)
	12.0	49.0	6.41 (0.23)	6.02 (0.17)	1.68 (0.05)	0.28 (0.008)	11.7 (0.42)	0.70 (0.02)
	15.7	32.7	2.49 (0.09)	7.45 (0.21)	2.03 (0.06)	0.26 (0.007)	14.1 (0.51)	0.51 (0.01)
SHA	N.A.[d]	N.A.	8.51 (0.31)	4.21 (0.12)	1.09 (0.03)	1.52 (0.043)	1.14 (0.04)	0.12 (0.01)
SRHA	N.A.	N.A.	7.13 (0.28)	9.67 (0.27)	1.25 (0.04)	0.73 (0.021)	4.02 (0.14)	0.26 (0.01)
SRFA	N.A.	N.A.	4.28 (0.15)	21.39 (0.60)	1.49 (0.04)	0.16 (0.005)	7.61 (0.27)	0.39 (0.01)

[a] The value was determined by synchronous fluorescence spectroscopy. [b] The values were determined by the specified peaks in fluorescence EEM (see the text). [c] Numbers in parentheses are standard errors based on propagating the corresponding measured value uncertainties. [d] Not applicable

step sizes, respectively. The fluorescence response to a blank solution (Milli-Q water) was subtracted from the three types of the fluorescence spectra to remove Raman scattering effects (Chen et al. 2003; McKnight et al. 2001). The EEMs were plotted using Sigma Plot 2000 (SPSS Inc.). No inner-filter correction was applied to the diluted samples. For this study, all the measured absorption and fluorescence spectra were normalized by the DOC to compare the spectroscopic characteristics and patterns of the samples at the same concentration level. Relative precisions of <2% were routinely obtained by 3-times repeated absorption and fluorescence measurements of randomly chosen samples. All of the DOC, absorption and fluorescence measurements were made within 24 h after the return from the field.

3 Results

3.1 Vertical variation of turbidity, temperature, DO, and DOC

Vertical profiles of turbidity showed that a turbid water layer was present at a middle depth of the reservoir between 10 and 20 m (Fig. 4a). The maximum turbidity per location reached 50–95 NTU (Nephelometric Turbidity Unit) and the value was greater downstream toward the dam, indicating that the turbid water moved downstream as the reservoir water was discharged through the outlet of the intake tower located near the dam. The turbidity data also suggest that the turbid water layer descended gradually toward the dam because the maximum value was found at a greater depth as the location is downstream from the station 4 to the station 1.

Vertical distribution of water temperature was different from a typical temperature pattern of a distinct thermocline in summer (Fig. 4b). Here, two thermal transition layers were observed with depth due to the formation of the new turbid water layer. Water temperature in the uppermost layer (i.e., epilimnion) exceeded 30°C and it declined to a depth where the turbid water layer is located. The temperature in the turbid water layer ranged from 15 to 20°C and it rapidly decreased again below the end depth of the turbid water layer. The steepest temperature gradient was typically observed at the

depth of approximately 22 m, the end of the turbid water layer.

A maximum DO concentration was observed in the upper layer due to the photosynthetic activities of algae. DO concentration decreased with depth (Fig. 4c). Below the upper layer, DO concentration appears to follow a relationship between DO concentration and temperature (i.e., higher DO concentration with lower water temperature), showing the opposite depth profile to the temperature. The observed DOC ranged from 1.4 to 2.1 mg C/L, with horizontal and vertical variations (Fig. 4d). Except for the station 1, DOC was the greatest in the turbid water layer and it declined with depth.

3.2 Ultraviolet absorbance ratio

For this study, a UV absorbance ratio of A_{254}/A_{436} was chosen as a UV–visible spectroscopic parameter of DOM to compare the absorption characteristics of the turbid water DOM with those of the surrounding reservoir DOM. The absorption ratio has been originally used to distinguish between allochthonous DOM and autochthonous DOM in river and lake water samples (Battin 1998; Hur et al. 2006; Jaffé et al. 2004). The selected wavelengths of the ratio (i.e., > 250 nm) are favorable because they are unlikely to be affected by the interferences of the anions present in field samples (Westerhoff et al. 2001). The absorbance ratios of the turbid water DOM exhibited much lower than those of other samples in the range between 5.0 and 7.5 (Table 1). In contrast, other samples exhibited the ratios greater than 10.0. The observed trend was consistent with a recent report of Hur et al. (2006), who demonstrated a decreasing absorbance ratio with higher content of a terrestrial humic acid (i.e., purified Aldrich humic acid) versus SRFA in the mixtures of the two DOM.

3.3 Fluorescence index (F_{450}/F_{500})

A ratio of fluorescence emission intensities at an excitation wavelength of 370 nm (F_{450}/F_{500}) has been typically used as a good index to identify DOM sources (autochthonous vs. allochthonous DOM) in lake and river samples (Battin 1998; McKnight et al. 2001). Higher fluorescence index corresponds to the relative abundance of autochthonous versus

Fig. 4 Vertical changes of turbidity (**a**), water temperature (**b**), dissolved oxygen (**c**), dissolved organic carbon (DOC) (**d**), and chlorophyll-a (**e**) of the sampling locations at the Yongdam Reservoir. Temperature, dissolved oxygen, and turbidity data were collected at the interval of 1 m using a YSI profiler. DOC and chlorophyll-a data were obtained from collected water samples. The *circled symbols* indicate the depths at which water samples were collected
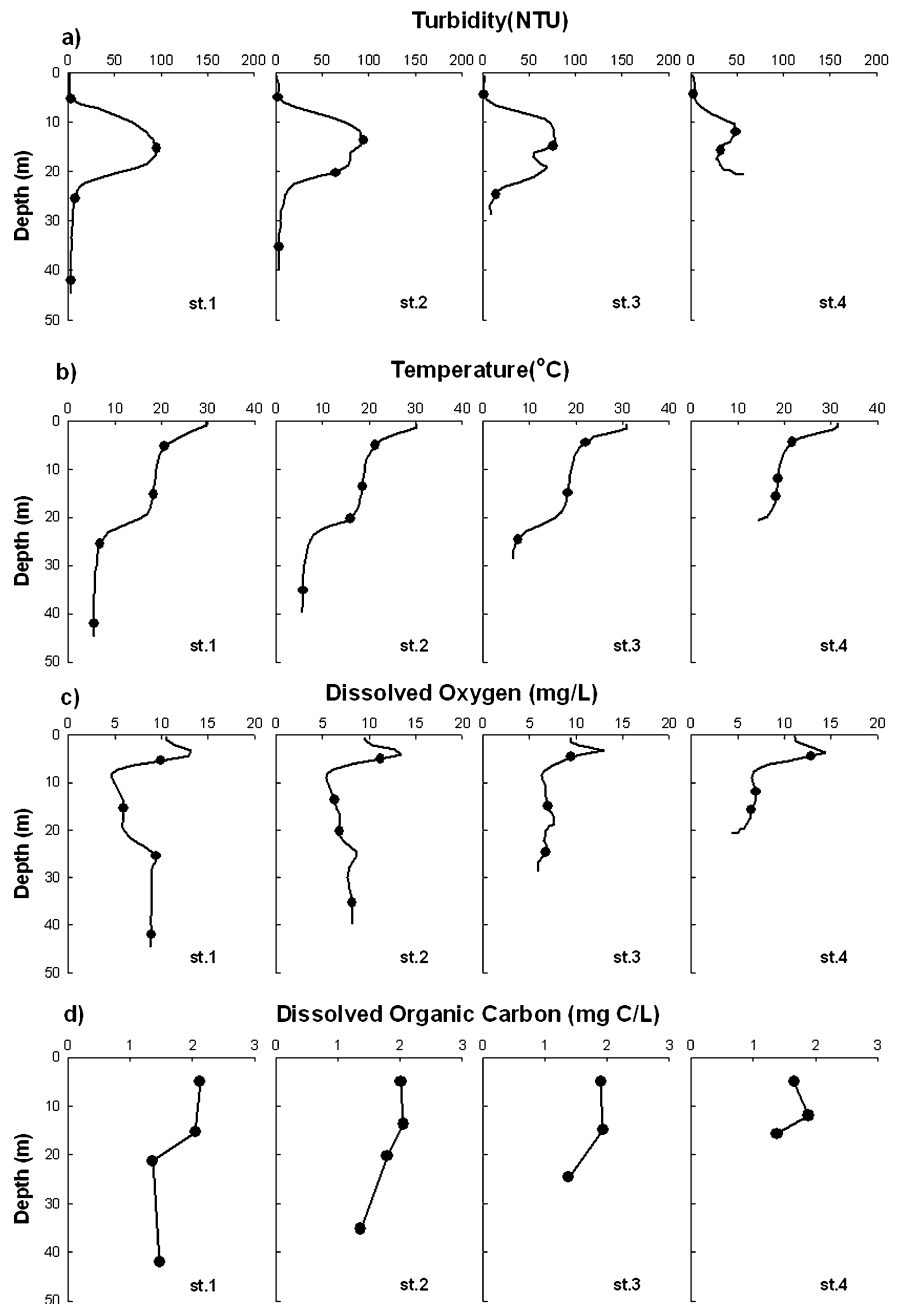
allochthonous DOM components. Our turbid water DOM samples could be easily distinguished from the surrounding reservoir samples by their fluorescence indices. The fluorescence index of the turbid water ranged from 1.63 to 1.75, which were lower than those of the surrounding reservoir DOM. Irrespective of the sampling location, the highest fluores-

cence index value was observed either in the upper layer, where algal activities are likely to be relatively high, or in the bottom layer where dead algae and the associated materials are accumulated and the subsequent decomposition may occur. The vertical variation of DOM composition expected from the fluorescence indices was consistent with

a previous study of Choi et al. (2001), who reported that a proportion of labile DOM (i.e., autochthonous DOM) was relatively low in the turbid water layer of the Soyang Reservoir in Korea.

3.4 Fluorescence spectral patterns

Several features of DOM fluorescence synchronous spectra have been originally suggested as indicators to distinguish DOM of different sources and to characterize DOM structural compositions (Jaffé et al. 2004; Lu et al. 2003; Peuravuori et al. 2002; Shin et al. 2001). Because synchronous fluorescence is affected by various factors such as solution chemistry of the sample and the offset value of the scan (i.e., $\Delta\lambda$) (Pullin and Cabaniss 1997), the fluorescence characteristics may not be consistently defined for a number of the studies. Nevertheless, a general trend of the DOM structural properties with wavelength was reported to be the same. For example, it is generally accepted that peaks appearing at longer wavelengths represent fulvic acid components with the lower degree of aromaticity whereas peaks at the longer wavelengths are associated with polycondensation of phenolic aromatic units such as humic acids (Chen et al. 2003; Ferranti and Mingazzini 1995; Lu et al. 2003; Miano and Senesi 1992). In Fig. 5a, synchronous fluorescence spectra of three IHSS standard DOM were compared to select appropriate wavelengths to distinguish humic-like and fulvic-like DOM composition from our field samples. The synchronous fluorescence spectrum of SRFA showed a major peak at 350 nm whereas two broad peaks were observed at around 400 and 450 nm for the two IHSS humic acids (SRHA and SHA). In contrast, our reservoir samples did not show such distinct characteristics. Instead, the spectrum shapes were similar to the mixtures of SRHA and SRFA. Some broad peaks at longer wavelengths (> ~420 nm) were more pronounced for the turbid water DOM, indicating that higher content of humic-like DOM components may be present in the turbid water layer versus other surrounding layers (Fig. 5b).

Fluorescence EEM provides an overall view of fluorescent properties of DOM in a selected spectral range and it has been employed to identify fluorescent compounds in DOM. Previous investigations have suggested that three fluorescence peaks such as humic-like, fulvic-like, and protein-like fluorescent compounds can be distinguished at different locations (Baker 2001; Chen et al. 2003; Coble 1996; Hur et al. 2006). For this study, different fluorescence spectral regions were assigned to each of the three fluorescent compound groups, following the definition proposed by Baker (2001). Protein-like fluorescence is present at 275 nm excitation and 350 nm emission wavelength, fulvic-like fluorescence at 320–340 nm excitation and 410–430 nm emission wavelength, and humic-like fluorescence at 370–390 nm excitation and 460–480 nm emission wavelength (Fig. 6). Of those characterized peaks, protein-like fluorescence has been most utilized to track dynamic changes of DOM composition in rivers, lakes and ocean (Baker 2001; Coble 1996; Levi et al. 2004; Parlanti et al. 2000; Yamashita and Tanoue 2003). For example, Parlanti et al. (2000) evaluated the biological activities and the degradation development of macro-algae in rivers and seawaters by monitoring the relative peak intensity of the protein-like fluorescence peak intensity versus other peaks in DOM samples. DOM samples in the Yongdam Reservoir showed dramatic changes of the fluorescence EEM spectral patterns with respect to the vertical and the horizontal locations (Figs. 6 and 7). The fulvic-like fluorescence peaks were commonly observed for all the DOM samples irrespective of the sampling location and the depth. In contrast, the protein-like fluorescence peak was observed only for non-turbid water DOM (i.e., the upper layer and the bottom layer).

3.5 Fluorescence ratios from synchronous spectra and EEM

Based on the previously reported DOM spectral features and the comparison of the IHSS DOM for this study, a ratio of synchronous fluorescence intensities at 450 and 350 nm was chosen to estimate the relative presence of humic-like and fulvic-like fluorescent DOM components in the reservoir samples. The synchronous fluorescence ratios were in the order of SHA > SRHA > turbid water DOM > SRFA ~ other reservoir samples (Table 1). The higher ratio of the turbid water DOM confirmed that the turbid water DOM originated from terrestrial sources. It is known that terrestrial DOM contains higher content

Fig. 5 Typical synchronous
spectra of the IHSS standard
materials including SHA,
SRHA, and SRFA (**a**) and
the Yongdam Reservoir
DOM at the station 2 (**b**)
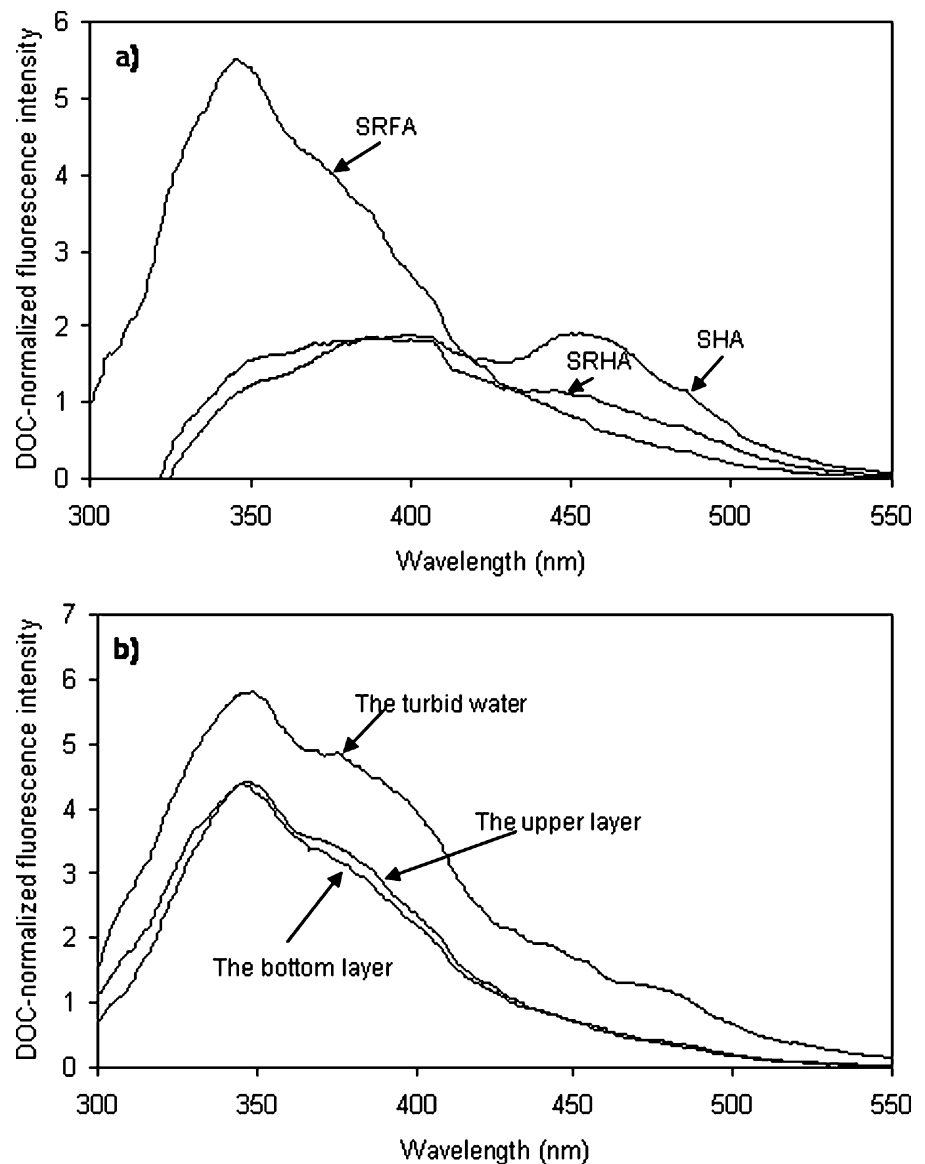
of humic acids versus fulvic acids compared to
aquatic DOM (Thurman 1985). The synchronous
fluorescence ratio in the upper layer decreased from
0.17 to 0.14 toward the dam (from the station 4 to the
station 1). This result is consistent with Balogh et al.
(2003), who reported a lower ratio of humic acid to
fulvic acid in DOM from surface water toward the
outlet of a large shallow lake along the longitudinal
axis. The ratio of the protein-like: the humic-like
fluorescence also showed vertical changes such that
the turbid water layer exhibited the lowest value at
each location. The ratio change was the most dramatic

near the dam site (the station 1), ranging from 0.6 to
12.3 (Table 1).

3.6 DOC-normalized spectroscopic parameters

SUVA has been widely applied to estimate aromatic
content of DOM. Chin et al. (1994) reported a
positive correlation between aromaticity and SUVA
values of aquatic DOM obtained from various
locations of lakes and rivers. SUVA values of all the
collected samples were compared to investigate the in-
fluence of the turbid water runoff on the distribution

Fig. 6 Fluorescence EEM spectra of the Yongdam Reservoir DOM (St. 1). (**a**) the upper layer, (**b**) the middle layer, (**c**) the turbid water layer, and (**d**) the bottom layer
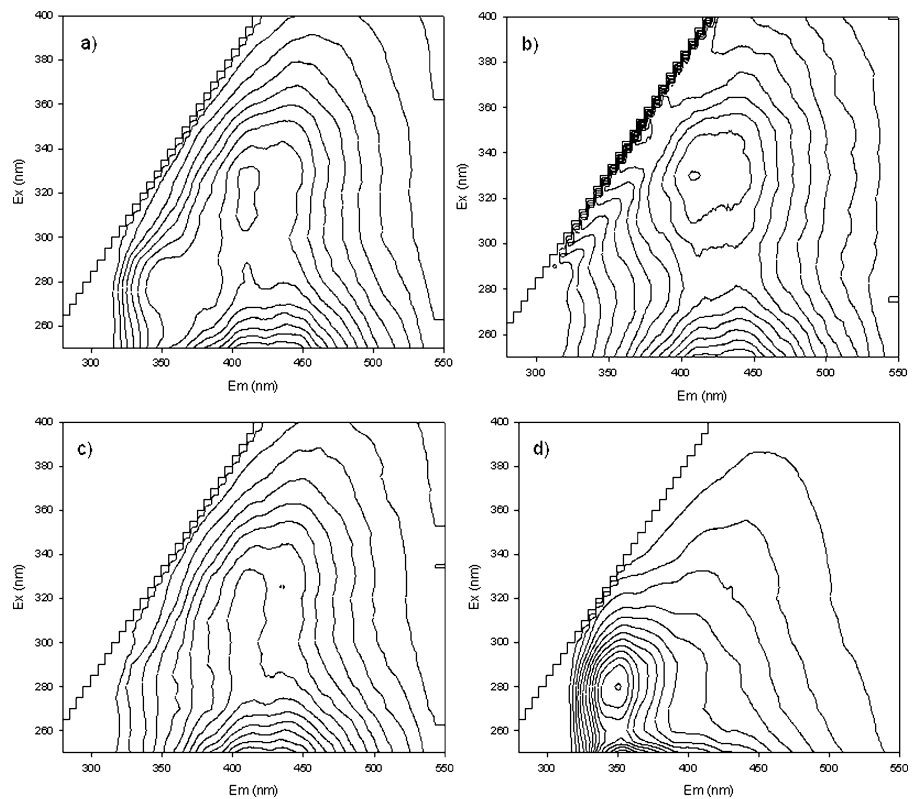
of aromatic DOM components (Table 1). For each sampling location, the SUVA value of the turbid water layer was the highest with the variation from 6.41 to 7.65, corresponding to a mixed range between SRFA and SHA. In contrast, DOM in the surrounding reservoir (the upper layer and the bottom layer) exhibited much lower SUVA values (2.43–3.05), which correspond to the intermediate range between the values of SRFA and algal-derived DOM (SUVA value=~1.0) extracted from blue-green algae reported by Her et al. (2004). This comparison suggests that allochthonous DOM constituted a major composition of DOM in both layers (the upper and the bottom) surrounding the turbid water of the reservoir. A positive linear correlation was observed between turbidity and the SUVA value of all the DOM samples for this study (R^2=0.86; data not shown). Our results were in general agreement with some prior studies. For example, Aiken and Cotsaris (1995) reported that DOM concentration and the aromaticity increased to approximately two and three times, respectively, the background levels during storm runoff events. Li et al. (2003) observed that SUVA value of DOM

in a river water increased from 1.8 to 2.9 on a heavy storm event.

DOC-normalized protein-like fluorescence intensities of our samples generally ranged from 7.9 to 20.4 except for the bottom layer near the dam (the station 1). The highest value was typically found in the bottom layer for each location (Fig. 7) whereas the turbid water exhibited the lowest value.

4 Discussion

4.1 Comparison of spectroscopic parameters

Compared to the surrounding reservoir water DOM, the turbid water DOM showed the lower and the higher value of A_{254}/A_{436} and SUVA, respectively. Based on the relative difference and the general trend between DOM sources/composition and the corresponding values reported in many previous literatures, our results suggest that the turbid water DOM contain more terrestrial-origin DOM composition. Our results also supported that the turbid water was flushed into
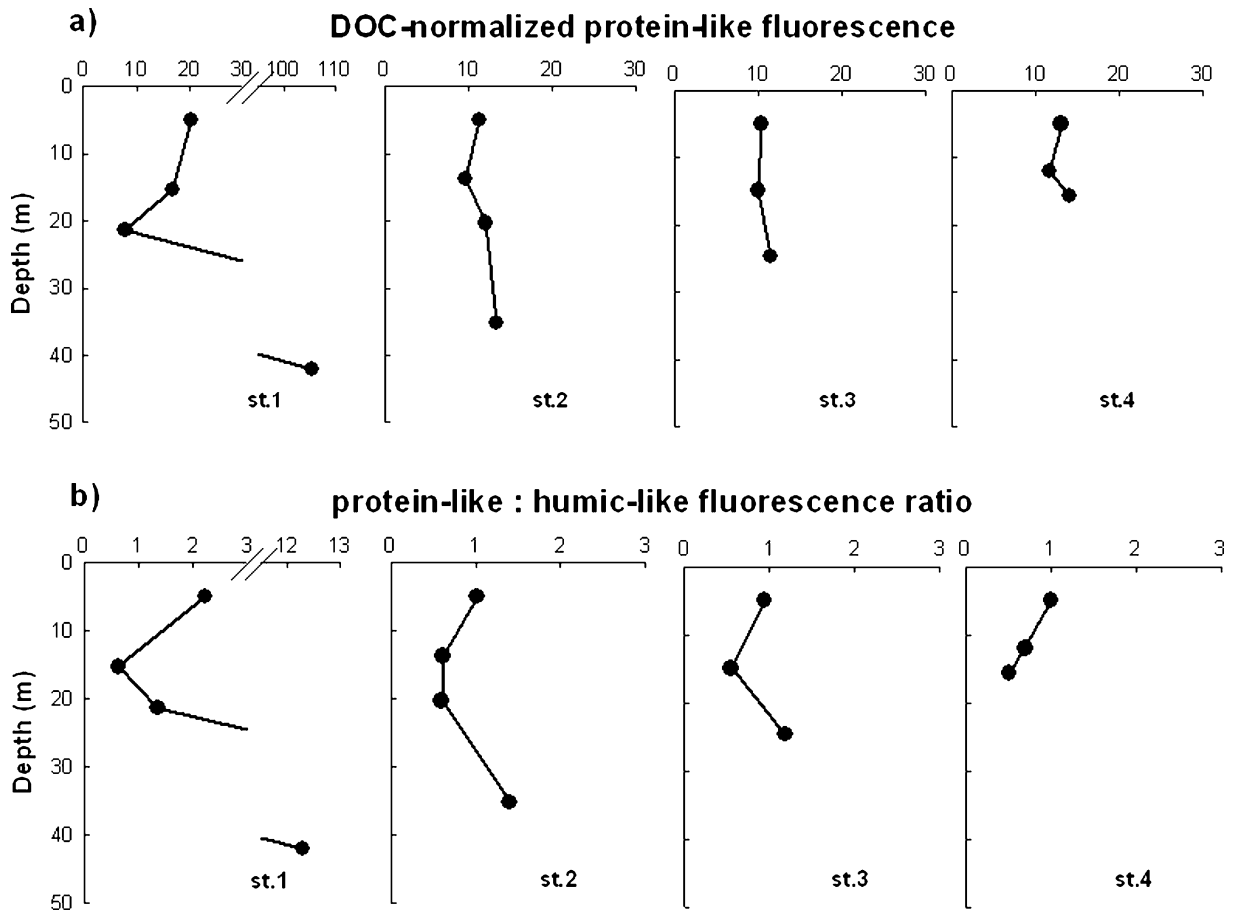
Fig. 7 Vertical changes of protein-like fluorescence (**a**) and the ratio of protein-like: humic-like fluorescence (**b**). The two fluorescence characteristics were quantified using fluorescence EEM information (see the text)

the reservoir from the catchment soils during the antecedent storm events. The capability of the SUVA value appears to be superior to the absorbance ratio of A_{254}/A_{436} for the source/composition discrimination, as evidenced by the lower R^2 value ($R^2 = 0.59$) of the correlation between the ratios and the turbidity data (Table 1). The distribution of the fluorescence characteristics such as the humic-like: fulvic-like fluorescence ratio and the DOC-normalized protein-like fluorescence intensity were also consistent with the trends expected from the source of the turbid water.

4.2 High protein-like fluorescence intensity of the bottom layer near the DAM

It is difficult to explain the extremely high protein-like fluorescence at the bottom layer near the dam.

The major source of the protein-like materials may include extracellular release from actively growing algae, autolysis of dead cells, microbial degradation of particulate organic detritus, and the leaching and the decomposition of the periphytons flushed with the turbid water on the antecedent storm events (Wetzel 2001). However, bacterial decomposition of the organic detritus is not likely to be very active at the low temperature of the bottom water (~5°C) because metabolic activities of bacteria are inversely correlated with water temperature (Wetzel 2001). In fact, the high content of the protein-like DOM composition in the bottom water conflicts with the vertical distribution of protein amino acids generally described in natural lakes, which depicts a maximum concentration in the epilimnion (Wetzel 2001; Wu and Tanoue 2001). A possible explanation for the observation is

that although the protein-like materials were originally produced in the upper layers, they were accumulated at the bottom layer due to sinking processes. Leaching from dead periphyton flushed into the reservoir at the storm events may also contribute the enrichment of the protein-like materials at the bottom. Once the protein-like DOM was accumulated at the bottom, it is likely to be well preserved under the low water temperature. However, the extremely high protein-like fluorescence was not seen at the bottom layer of the station 3 despite the same low temperature. It is necessary to note that the reservoir water is discharged through the reservoir outlet and therefore that a horizontal movement of the entire reservoir water constantly takes place towards the dam (Fig. 3). For the Yongdam Reservoir, the outlet is located on the upper part of the intake tower (the opening extends to the depth of 8 m below the surface water level). The outlet location may isolate the local bottom water from the entire reservoir water, preventing it from being discharged through the outlet (Shin et al. 2004). In addition, this effect would be more pronounced as the sampling location is closer to the withdrawal outlet near the dam (Fig. 3). The accumulated protein-like DOM component near the dam could be partially discharged when the thermocline is broken in winter (i.e., turnover). Our spectroscopic results demonstrated that the distribution of DOM composition in a dam reservoir may be strongly affected by the outflow operation of the dam such as selective withdrawal as well as terrestrial DOM inputs from intense storm runoff.

4.3 Limitations of spectroscopic characterization in this study

Although most of the particulate matters in the field sample were removed from the samples after filtration, colloidal particles may still be present in the filtrates and they might affect the SUVA values and the absorbance ratios of the samples due to light scattering. For example, Karanfil et al. (2005) reported that UV absorbance at 254 nm was greater than it should be when the filtrate turbidity was > 0.5 NTU. Therefore, it is probable that both high turbidity and terrestrial DOM inputs together contributed the notable ultraviolet characteristics of the filtered turbid water. In contrast to the ultraviolet absorbance, fluorescence intensities of DOM are not significantly affected by the presence of colloidal particles. For example, Lee and Ahn (2004) compared fluorescence intensities of filtered wastewater effluent samples versus the unfiltered samples with suspended solid concentrations ranging from 10 to 60 mg/L, and they reported similar fluorescence properties.

Colorless components of DOM were not considered in this study due to the inherent limitation of spectroscopic characterization. It should be noted, however, that the spectroscopic measurements is still useful to track changes of DOM composition. For example, Yamashita and Tanoue (2003) reported that protein-like fluorescence intensity in fluorescence EEM was positively correlated with total hydrolysable amino acid concentration and they demonstrated that the protein-like fluorescence could be used to quantify not only the aromatic fraction of the amino acids in DOM but also the total amount of amino acids.

Another thing one should note in using the spectroscopic measurements as a tool to track changes of DOM composition is that the absorption and the fluorescence characteristics of the original DOM may be changed by photochemical alternation. Hayakawa et al. (2004) observed that the humic-like fluorescence intensity from EEM of lake DOM decayed during photobleaching.

5 Conclusions

Spectroscopic characteristics of DOM in the turbid water layer in the Yongdam Reservoir were different from those of the surrounding layers (the upper and the bottom layers), suggesting that the distribution of DOM composition in the reservoir was impacted by the turbid storm runoff. Terrestrial DOM characteristics were more observed for the turbid water DOM versus the surrounding reservoir DOM as revealed by the higher SUVA values and the lower A_{254}/A_{436} absorbance ratio. Fluorescence analyses also supported the terrestrial origin of the turbid water DOM as demonstrated by a greater ratio of humic-like to fulvic-like fluorescence ratio and low protein-like fluorescence. The fluorescence results showed that extremely high content of the protein-like fluorescent DOM was exclusively present at the bottom layer near the dam site. This observation was explained by the accumulation of the sinking protein-like DOM

materials originally produced in the upper layer and the isolation of the local dam bottom water due to the upper location of the withdrawal outlet. This study demonstrated that the distribution of DOM composition in a dam reservoir might be strongly affected by the outflow operation, such as a selective withdrawal of the dam reservoir and terrestrial DOM input from storm runoff.

References

Aiken, G., & Cotsaris, E. (1995). Soil and hydrology: Their effect on NOM. *Journal American Water Works Association, 1995*, 36–45.

Alberts, J. J., & Takács, M. (2004). Total luminescence spectra of IHSS standard and reference fulvic acids, humic acids, natural organic matter: Comparison of aquatic and terrestrial source terms. *Organic Geochemistry, 35*, 243–256.

Baker, A. (2001). Fluorescence excitation–emission matrix characterization of some sewage-impacted rivers. *Environmental Science & Technology, 35*, 948–953.

Balogh, K. V., Vörös, L., Tóth, N., & Bokros, M. (2003). Changes of organic matter quality among the longitudinal axis of a large shallow lake (Lake Balaton). *Hydrobiologia, 506–509*, 67–74.

Battin, T. J. (1998). Dissolved organic matter and its optical properties in a blackwater tributary of the upper Orinoco river, Venezuela. *Organic Geochemistry, 28*(9/10), 561–569.

Chen, W., Westerhoff, P., Leenheer, J. A., & Booksh, K. (2003). Fluorescence excitation–emission matrix regional integration to quantify spectra for dissolved organic matter. *Environmental Science & Technology, 37*, 5701–5710.

Chen, Y. J. C., Wu, S. C., Lee, B. S., & Hung, C. C. (2006). Behavior of storm-induced suspension interflow in subtropical Feitsui Reservoir, Taiwan. *Limnology and Oceanography, 51*, 1125–1133.

Chin, Y.-P., Aiken, G., & O'Loughlin, E. (1994). Molecular weight, polydispersity, and spectroscopic properties of aquatic humic substances. *Environmental Science & Technology, 28*, 1853–1858.

Choi, K., Kim, B., & Lee, U. (2001). Characteristics of dissolved organic carbon in three layers of a deep reservoir, Lake Soyang, Korea. *International Review of Hydrobiology, 86*, 63–76.

Coble, P. G. (1996). Characterization of marine and terrestrial DOM in seawater using exciation–emission matrix spectroscopy. *Marine Chemistry, 51*, 325–346.

Ferranti, G. M., & Mingazzini, M. (1995). Synchronous fluorescence spectra of dissolved organic matter (DOM) of algal origin in marine coastal waters. *Marine Ecology Progress Series, 125*, 305–315.

Hayakawa, K., Sakamoto, M., Kumagai, M., Jiao, C., Song, X., & Zhang, Z. (2004). Fluorescence spectroscopic characterization of dissolved organic matter in the water of Lake Fuxian and adjacent rivers in Yunnan, China. *Limnology, 5*, 155–163.

Her, N., Amy, G., Park, H.-R., & Song, M. (2004). Characterizing algogenic organic matter (AOM) and evaluating associated NF membrane fouling. *Water Research, 38*, 1427–1438.

Hur, J., Williams, M. A., & Schlautman, M. A. (2006). Evaluating spectroscopic and chromatographic techniques to resolve dissolved organic matter via end member mixing analysis. *Chemosphere, 63*, 387–402.

Jaffé, R., Boyer, J. N., Lu, X., Maie, N., Yang, C., Scully, N. M., et al. (2004). Source characterization of dissolved organic matter in a subtropical mangrove-dominated estuary by fluorescence analysis. *Marine Chemistry, 84*, 195–210.

Karanfil, T., Erdogen, I., & Schlautman, M. A. (2005). The impact of filtrate turbidity on UV_{254} and $SUVA_{254}$ determinations. *Journal American Water Works Association, 97*(5), 125–136.

Kim, B., Choi, K., Kim, C., Lee, U., & Kim, Y. (2000). Effects of the summer monsoon on the distribution and loading of organic carbon in a deep reservoir, Lake Soyang, Korea. *Water Research, 34*(14), 3495–3504.

Lee, S., & Ahn, K.-H. (2004). Monitoring of COD as an organic indicator in wastewater and treated effluent by fluorescence excitation–emission (FEEM) matrix characterization. *Water Science and Technology, 50*(8), 57–63.

Levi Cammack, W. K., Klaff, J., Prairie, Y. T., & Smith, E. M. (2004). Fluorescent dissolved organic matter in lakes: Relationships with heterotrophic metabolism. *Limnology and Oceanography, 49*(6), 2034–2045.

Li, F., Yuasa, A., Chiharada, H., & Matsui, Y. (2003). Storm impacts upon the composition of organic matricies in Nagara River – A study based on molecular weight and activated carbon adsorbability. *Water Research, 37*, 4027–4037.

Lu, X. Q., Maie, N., Hanna, J. V., Childers, D. L., & Jaffé, R. (2003). Molecular characterization of dissolved organic matter in freshwater wetlands of the Florida Everglades. *Water Research, 37*, 2599–2606.

McKnight, D. M., Boyer, E. W., Westerhoff, P. K., Doran, P. T., Kulbe, T., & Andersen, D. T. (2001). Spectrofluorometric characterization of dissolved organic matter for indication of precursor organic material and aromaticity. *Limnology and Oceanography, 46*, 38–48.

Miano, T. M., & Senesi, N. (1992). Synchronous excitation fluorescence spectroscopy applied to soil humic substances chemistry. *Science of the Total Environment, 117*, 41–51.

Mobed, J. J., Hemmingsen, S. L., Autry, J. L., & McGown, L. B. (1996). Florescence characterization of IHSS humic substances: Total luminescence spectra with absorbance correction. *Environmental Science & Technology, 30*, 3061–3065.

Parlanti, E., Wörz, K., Geoffroy, L., & Lamotte, M. (2000). Dissolved organic matter fluorescence spectroscopy as a tool to estimate biological activity in a coastal zone submitted to anthropogenic inputs. *Organic Geochemistry, 31*, 1765–1781.

Peuravuori, J., Koivikko, R., & Pihlaja, K. (2002). Character-ization, differentiation and classification of aquatic humic matter separated with different sorbents: Synchronous scanning fluorescence spectroscopy. *Water Research, 36*, 4552–4562.

Pullin, M. J., & Cabaniss, S. T. (1997). Physicochemical variations in DOM-synchronous fluorescence: Implications for mixing studies. *Limnology and Oceanography, 42*(8), 1766–1773.

Shin, H., Hong, K., Lee, M., Cho, Y., & Lee, C. (2001). Fluorescence quenching of three molecular weight fractions of a soil fulvic acid by $UO_2(II)$. *Talanta, 53*, 791–799.

Shin, J. K., Jeong, S. A., Choi, I., & Hwang, S. J. (2004). Dynamics of turbid water in a Korean reservoir with selective withdrawal discharges. *Korean Journal of Limnology, 37*(4), 423–430.

Steinberg, C. E. W. (2003). *Ecology of humic substances in freshwaters*. Berlin Heidelberg New York: Springer.

Thurman, E. M. (1985). *Organic geochemistry of natural waters*. Dordrecht, The Netherlands: Martinus Nijhoff/Junk.

Westerhoff, P., Chen, W., & Esparza, M. (2001). Fluorescence analysis of a standard fulvic acid and tertiary treated waste-water. *Journal of Environmental Quality, 30*, 2037–2046.

Wetzel, R. G. (2001). *Limnology: Lake and river ecosystems*. New York: Elsevier.

Wu, F., & Tanoue, E. (2001). Geochemical characterization of organic ligands for copper (II) in different molecular size fractions in Lake Biwa, Japan. *Organic Geochemistry, 32*, 1311–1318.

Wu, F. C., Tanoue, E., & Liu, C. Q. (2003). Fluorescence and amino acid characteristics of molecular size fractions of DOM in the waters of Lake Biwa. *Biogeochemistry, 65*, 245–257.

Yamashita, Y., & Tanoue, E. (2003). Chemical characterization of protein-like fluorophores in DOM in relation to aromatic amino acids. *Marine Chemistry, 82*, 255–271.